plants

MDPI

Article

Influence of Local Burning on Difference Reflectance Indices Based on 400–700 nm Wavelengths in Leaves of Pea Seedlings

Ekaterina Sukhova *[ID], Lyubov Yudina [ID], Ekaterina Gromova, Anastasiia Ryabkova, Vladimir Vodeneev [ID] and Vladimir Sukhov [ID]

Department of Biophysics, N.I. Lobachevsky State University of Nizhny Novgorod,
603950 Nizhny Novgorod, Russia; lyubovsurova@mail.ru (L.Y.); kater333@inbox.ru (E.G.);
nastay2903@bk.ru (A.R.); v.vodeneev@mail.ru (V.V.); vssuh@mail.ru (V.S.)
* Correspondence: n.catherine@inbox.ru; Tel.: +7-929-040-2938

Abstract: Local damage (e.g., burning) induces a variation potential (VP), which is an important electrical signal in higher plants. A VP propagates into undamaged parts of the plant and influences numerous physiological processes, including photosynthesis. Rapidly increasing plant tolerance to stressors is likely to be a result of the physiological changes. Thus, developing methods of revealing VP-induced physiological changes can be used for the remote sensing of plant systemic responses to local damage. Previously, we showed that burning-induced VP influenced a photochemical reflectance index in pea leaves, but the influence of the electrical signals on other reflectance indices was not investigated. In this study, we performed a complex analysis of the influence of VP induction by local burning on difference reflectance indices based on 400–700 nm wavelengths in leaves of pea seedlings. Heat maps of the significance of local burning-induced changes in the reflectance indices and their correlations with photosynthetic parameters were constructed. Large spectral regions with significant changes in these indices after VP induction were revealed. Most changes were strongly correlated to photosynthetic parameters. Some indices, which can be potentially effective for revealing local burning-induced photosynthetic changes, are separately shown. Our results show that difference reflectance indices based on 400–700 nm wavelengths can potentially be used for the remote sensing of plant systemic responses induced by local damages and subsequent propagation of VPs.

Keywords: variation potential; reflectance indices; photosynthetic response; remote sensing; pea leaves

1. Introduction

Local actions of stressors on plants require systemic adaptive responses based on the generation and propagation of long-distance stress signals. Electrical signals (ESs), including action potential, system potential, and variation potential (VP) [1–9], play an important role in the induction of physiological changes in non-irritated parts of plants. It is known that an action potential is a self-propagating depolarization electrical signal [1–3,6,10] induced by non-damaging stimuli and is caused by both transient activation of Ca^{2+}, K^+, and anion channels, and inactivation of H^+-ATPase in the plasma membrane. The system potential is a weakly investigated hyperpolarization signal [8,11,12] caused by transient activation of H^+-ATPase and, possibly, changes in activity K^+ channels.

A VP is a long-distance signal in higher plants induced by local damage [2,4,6,13], which is formed by long-term depolarization and short-term "AP-like" spikes. The generation of a VP is mainly based on transient inactivation of H^+-ATPase, induced by Ca^{2+} influx through Ca^2 channels [2,13], but anion and outward K^+ channels can participate in the generation of AP-like spikes [4]. The mechanisms of VP propagation are still being discussed. The first hypothesis [13–16] supposes that a VP is a local electrical response induced by a hydraulic wave, which propagates through a plant from the damaged zone and activates mechanosensitive Ca^{2+} channels. The second hypothesis [4,17] supposes that

the VP is the local electrical response induced by the propagation of a specific "wound substance" from the damaged zone and the activation of ligand-dependent Ca^{2+} channels. Additionally, there are hypotheses of VP propagation based on combinations of hydraulic and chemical signals [18–21].

ESs induced by local stimuli can strongly influence physiological processes in non-irritated parts of plants [2,3,5,7,8]. It is known that ESs increase the expression of defense genes [22–25], respiration [26–28], ATP content in leaves [28], production of phytohormones [9,25,29–32], etc. In contrast, other physiological processes (e.g., phloem loading [33], phloem mass flow [34,35], and plant growth [36]) can be suppressed after propagation of ESs. Photosynthesis is an important target of ESs [5]. It is known that ESs decrease photosynthetic CO_2 assimilation, quantum yield of photosystem I, quantum yield of photosystem II (Y(II)), and mesophyll CO_2 conductance [23,27,37–43]. Non-photochemical quenching of chlorophyll fluorescence (NPQ), cyclic electron flow, and photosynthetic light absorption can be stimulated by ESs [27,37,39,43–45]. Increasing plant tolerance to stressors (including tolerance of photosynthetic machinery) is likely the result of physiological changes [46–53].

It can be expected that monitoring of electrical activity and ES-induced physiological changes is a potential tool for revealing the actions of stressors on plants. Investigations of plant electrical activity show that (i) the total electrical activity of plants ("electrome") can be strongly dependent on abiotic and biotic factors [53–57], and (ii) analysis of the electrical activity can be used for the classification of stressors that act on plants [58–62]. However, direct measurements of electrical activity cannot be used for the remote sensing of ES-induced systemic responses because electrodes would need to be connected to the plant. An alternative approach can be based on revealing relationships between ES-induced physiological changes and changes in plant reflectance. Previously, we showed that ESs induce changes in broadband reflectance indices [63,64] and decrease some narrowband indices, including the water index [64], which shows the water content in leaves, and the photochemical reflectance index (PRI) [65]. The PRI is strongly related to photosynthetic processes [66–74], including Y(II) and NPQ [75–77]. Its fast changes (seconds and minutes) are caused by the acidification of a chloroplast lumen through transitions in the xanthophyll cycle [66,68,78] and a change in light scattering at 530–546 nm [68,77], which is likely to be caused by chloroplast shrinkage [75,77]. It is known that ESs are accompanied by pH decreases in the cytoplasm, stroma, and lumen [38,39,79]; the luminal pH decrease is likely to be a mechanism of the ES's influence on the PRI.

However, using only the current narrowband reflectance indices (RIs) can limit the search for new RIs that are sensitive to the ES-induced physiological changes, because the reflected light at most wavelengths is not analyzed in standard RIs. The limitation can be eliminated by using heat maps showing (i) the correlation coefficients of physiological parameters to all possible RIs calculated on the basis of measured spectra [80–82] or (ii) the significance of changes in these RIs under the action of stressors [83]. Considering these approaches, it can be expected that a similar analysis of RIs in the 400–700 nm spectral range, which is related to photosynthetic processes, could reveal new RIs that are sensitive to ES-induced photosynthetic changes.

The aim of the current work was to perform a complex analysis of the influence of local burning, which is a typical inductor of VP (a key ES in higher plants [5,8]), on difference reflectance indices based on 400–700 nm wavelengths in leaves of pea seedlings. The analysis was based on spectra and photosynthetic parameters, which were preliminarily measured in our work [65] devoted to VP influence on the PRI. The spectra were used for the calculation of all probable RIs, and their changes after VP induction and correlations with photosynthetic parameters were investigated.

2. Data Analysis

2.1. General Scheme of Data Analysis

We used spectral and photosynthetic data from [65] in our analysis. Only data taken from the second leaf were analyzed, because the local burning-induced electrical signals and

photosynthetic and PRI changes in the fourth leaf [65] were weak. All spectra of reflected light and photosynthetic parameters measured in the second leaves were analyzed as a single experimental group (i.e., similar experimental groups from [65] were combined into one group). This group included 13 repetitions.

Figure 1 shows the scheme of the data analysis. Seven time points were used, including two points before VP induction (15 and 5 min before) and five points after the induction (5, 15, 25, 35, and 45 min after). We previously showed that RIs calculated on the basis of 400–700 nm wavelengths can have non-normal distributions [83]. Thus, we used non-parametric statistics in our analysis. Medians of the investigated values were used as the non-parametric analog of averaged values.
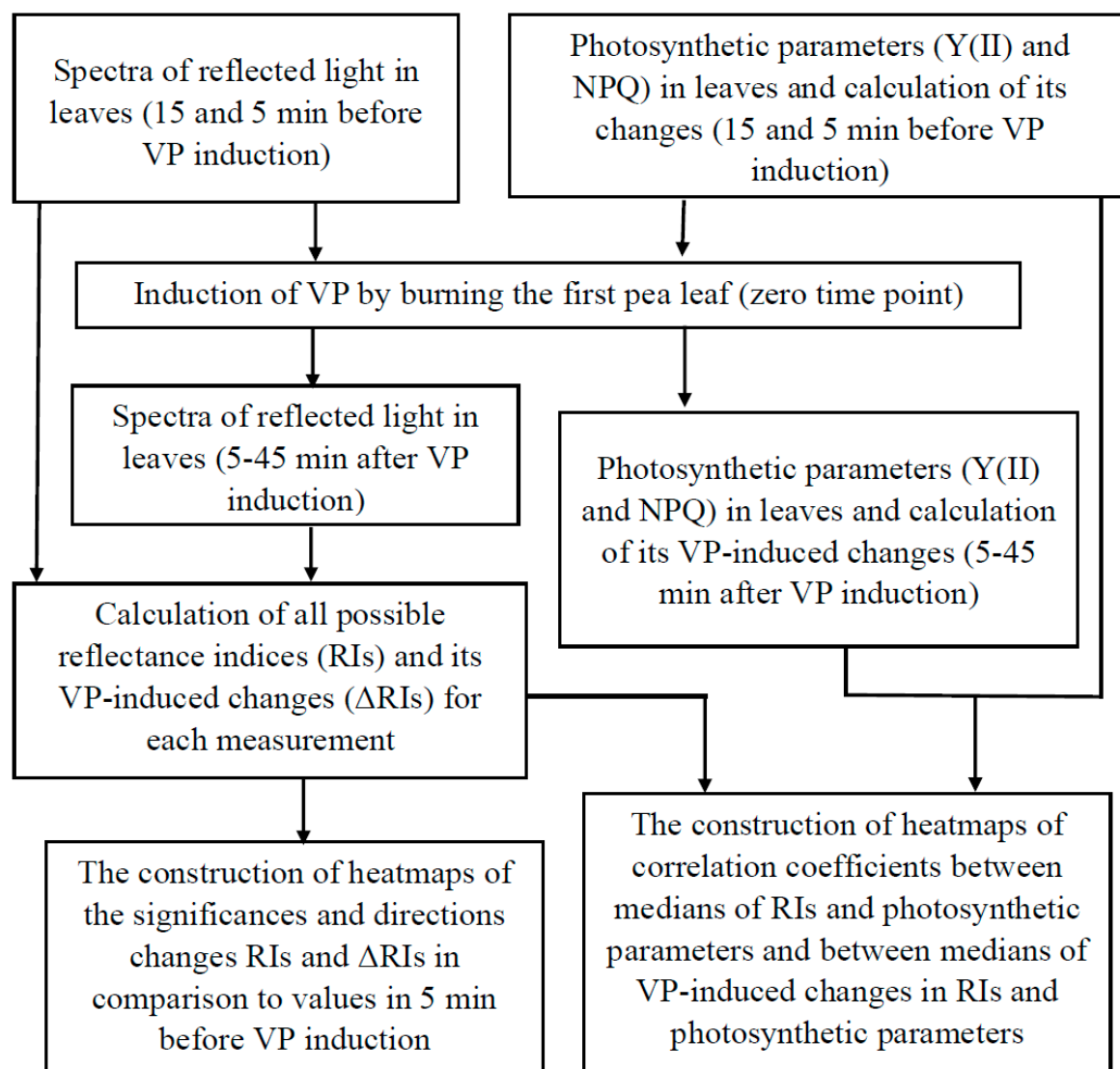
Figure 1. General scheme of analysis of spectra of the reflected light and photosynthetic parameters (the quantum yield of photosystem II, Y(II), and non-photochemical quenching of chlorophyll fluorescence, NPQ) measured in the second pea leaf before and after induction of variation potential (VP) by local burning of the first leaf.

The values of the investigated parameters 5 min before VP induction were used as control values for each plant. We calculated the absolute values of the investigated parameters (RIs, Y(II), and NPQ) and their changes (differences between current and control values of the parameters in each plant, ΔRIs, ΔY(II), and ΔNPQ). Significant differences between values were calculated using the non-parametric Mann–Whitney

U test. Relationships between reflectance indices and photosynthetic parameters were estimated on the basis of Pearson's correlation coefficients. Medians, which were separately calculated on the basis of the absolute values of the parameters or their changes for each time point, were used for the calculation ($n = 7$).

2.2. Calculation of Difference Reflectance Indices and Construction of Heat Maps

The calculation of RIs (or ΔRIs) and the construction of heat maps were based on several programs, which were developed using the Python 3.8 programming language. They solved the following tasks:

(i) Calculation of all possible RIs on the basis of Equation (1):

$$\mathrm{RI} = \frac{\mathrm{I(R_1)} - \mathrm{I(R_2)} \frac{\mathrm{I_C(R_1)}}{\mathrm{I_C(R_2)}}}{\mathrm{I(R_1)} + \mathrm{I(R_2)} \frac{\mathrm{I_C(R_1)}}{\mathrm{I_C(R_2)}}}, \tag{1}$$

where $\mathrm{I(R_1)}$ and $\mathrm{I(R_2)}$ are the intensities of the reflected light from a leaf at R_1 and R_2 wavelengths, respectively; $\mathrm{I_C(R_1)}$ and $\mathrm{I_C(R_2)}$ are the intensities of the reflected light from a white reflectance standard at R_1 and R_2 wavelengths (in accordance with [76,84]), respectively. To increase accuracy, averaged intensities of reflected light (3 nm range) were used. RIs were not calculated at $R_2 \geq R_1$. Changes in RIs (ΔRIs) were calculated according to Equation (2):

$$\Delta\mathrm{RI} = \mathrm{RI_{TP}} - \mathrm{RI_C}, \tag{2}$$

where $\mathrm{RI_{TP}}$ is the RI at a specific time point, and $\mathrm{RI_C}$ is the control RI equal to the RI at 5 min before VP induction.
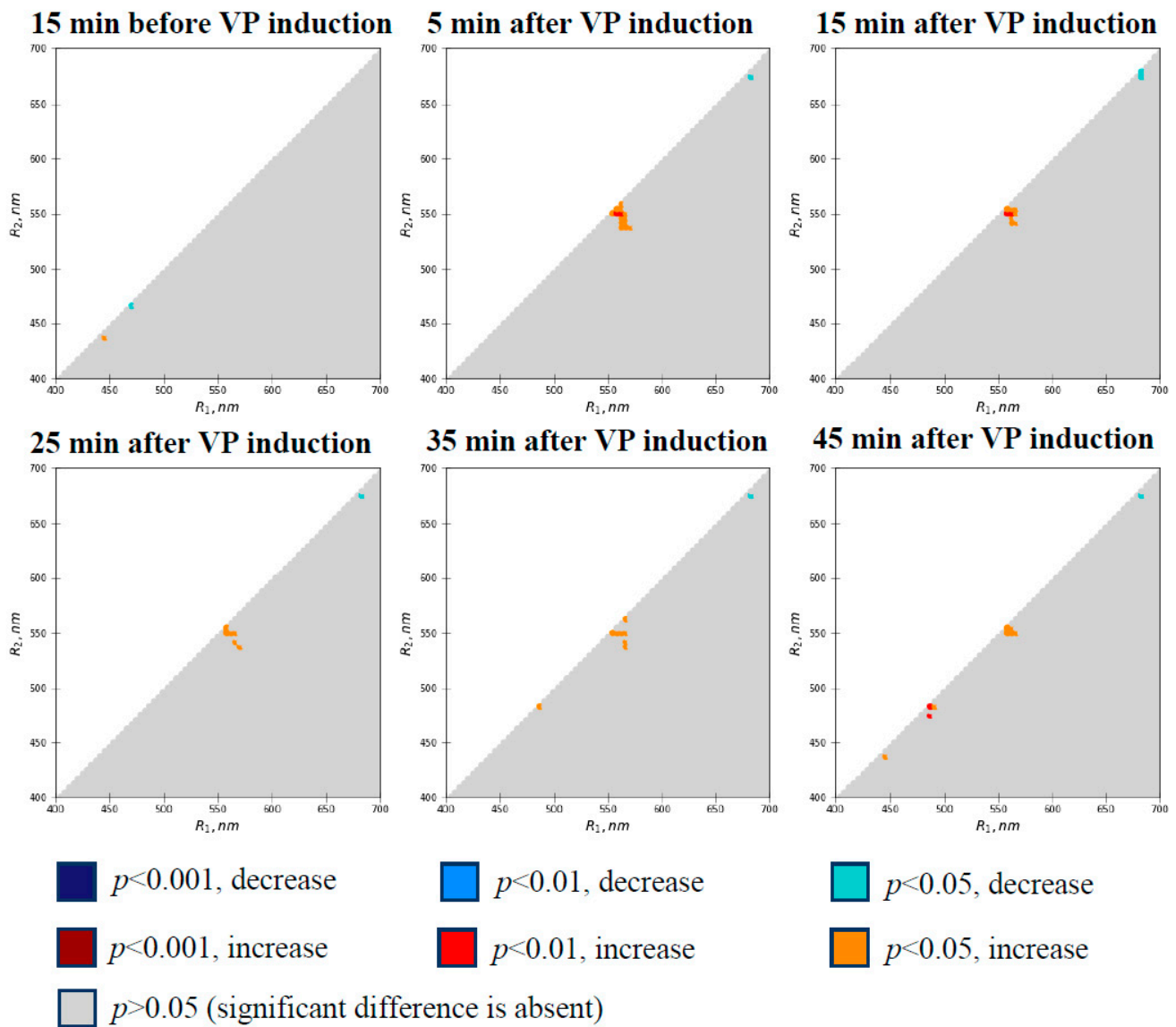
(ii) Calculation of the significance (p) of differences between experimental and control values of RIs (or ΔRIs) on the basis of the non-parametric Mann–Whitney U test and estimation of the directions of the differences. Two-dimensional data arrays (significance and directions of changes for each RI as a function of R_1 and R_2) were used for the construction of heat maps.

(iii) Calculation of the medians of RIs (or ΔRIs) at each time point and Pearson's correlation coefficients of these medians to similar medians of Y(II) and NPQ. Two-dimensional data arrays (correlation coefficients for each RI as a function of R_1 and R_2) were used for the construction of heat maps.

3. Results

3.1. Local Burning-Induced Changes in Difference Reflectance Indices

Figure 2 shows the heat maps of the significance and directions of differences between the absolute values of RIs at different time points and the control values. It is shown that differences were absent in the RIs before VP induction. Induction of a VP by local burning caused a transient increase in RIs (mostly at 5 and 15 min after heating) in a small spectral range (R_1 was about 550–570 nm; R_2 was about 535–560 nm). The increase in RIs approximately corresponded to the decrease in the PRI, which was shown in [65]. The opposite direction of RI changes is related to the opposite order of R_1 and R_2, because the PRI based on $R_1 = 531$ nm and $R_2 = 570$ nm [65] corresponds to the RI based on $R_1 = 570$ nm and $R_2 = 531$ nm in Figure 2. It is interesting that there were extremely small areas (pixel level) showing significant changes in RIs in other spectral ranges (e.g., RIs based on R_1 equal to about 680 nm and R_2 equal to about 675 nm; the measured reflected light at the wavelengths can additionally include chlorophyll fluorescence).
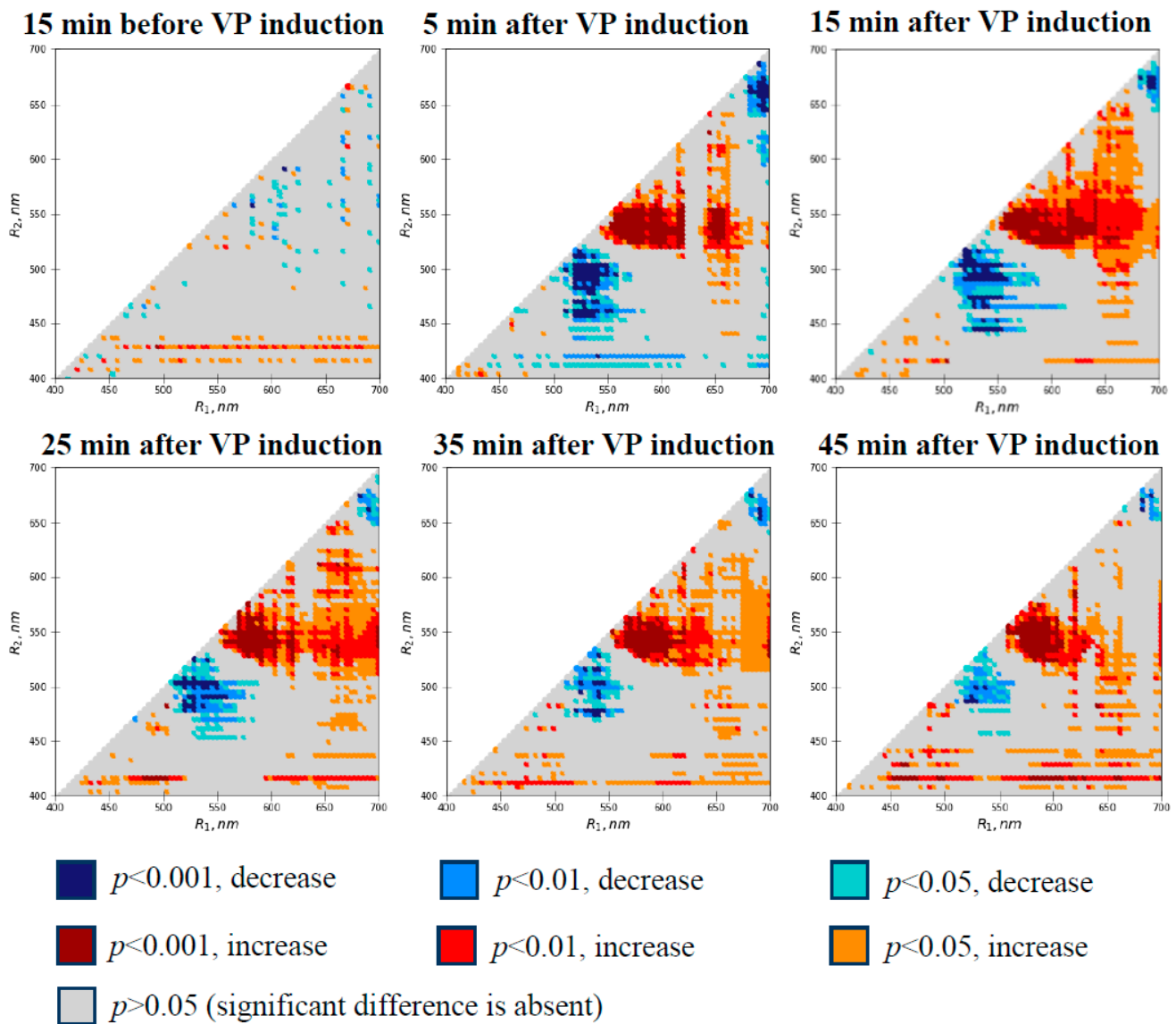
Figure 2. Heat maps of significance and directions of changes in absolute values of RIs in the second pea leaf at different time intervals before and after induction of variation potential (*n* = 13). RIs were calculated based on Equation (1). Burning of the first leaf was used for VP induction. The Mann–Whitney U test was used for *p*-value calculations. The absolute values of RIs were compared to the values of RIs at 5 min before VP induction.

Previously, we showed that changes in RIs (e.g., PRI or broadband reflectance indices) were more sensitive to short-term actions of stressors [63–65,76,83,85] than their absolute values, because using ΔRIs excluded the individual variability of the initial values of RIs and decreased the standard errors of the measured values. The effect was also observed in works by other authors (e.g., [74,86] for PRI). Thus, we analyzed the significance of the changes in ΔRIs in a further analysis and constructed heat maps of the significance of changes in ΔRIs (Figure 3).

There were only separate pixels on the first heat map showing a significant difference in ΔRIs at 15 min before VP induction (Figure 3). The localizations of the pixels were rather chaotic, excluding a few pixel lines in the lower part of the figure. It is also important to note that RIs with highly significant differences (*p* < 0.001) were practically absent in the variants (about 0.1% of the total quantity of RIs). Considering these results, we supposed that the changes in RIs were mainly related to revealing false changes, which were caused by stochastic differences in the spectra measured at different time intervals

and the large quantity of simultaneously analyzed RIs. The false changes could be the result of cooperative effects of moderate stochastic differences in light measurements at both wavelengths (separate pixels) or high stochastic differences at a single wavelength (line of pixels).

Figure 3. Heat maps of significance and directions of changes in ΔRIs in the second pea leaf at different time intervals before and after induction of variation potential (n = 13). RIs were calculated based on Equation (1). Burning of the first leaf was used for VP induction. Each ΔRI was calculated as RI_{TP}–RI_C. RI_C is the control RI at 5 min before the VP induction. RI_{TP} is the difference in the reflectance index at a specific time point before or after VP induction. The Mann–Whitney U test was used for p-value calculations. The ΔRIs were compared to zero values (absence of changes). Using ΔRIs minimized the influence of individual plant differences on the local burning-induced changes in RIs.

VP induction by local burning strongly influenced ΔRIs (Figure 3). There were several large spectral regions in the heat maps with significant positive changes in ΔRIs (e.g., R_1 was about 540–625 nm and R_2 was about 520–560 nm), in addition to negative changes (e.g., R_1 was about 510–560 nm and R_2 was about 450–520 nm). The area of the spectral regions was dependent on the duration after VP induction. For example, ΔRIs with highly significant changes ($p < 0.001$) accounted for 8–9% of the total quantity of ΔRIs at 5 and 15 min after burning and for approximately 4–5% at 35 and 45 min.

The results show that the induction of VP by local burning caused changes in a large number of ΔRIs and weakly influenced the absolute values of RIs. The changes could be related to local burning-induced photosynthetic changes in pea leaves; as a result, an analysis of the relations of RIs and ΔRIs to photosynthetic parameters was the next task of investigation.

3.2. Relations of Local Burning-Induced Changes in Difference Reflectance Indices to Changes in Photosynthetic Parameters

Figure 4 shows the absolute values of Y(II) and NPQ and changes in the parameters (ΔY(II) and ΔNPQ) before and after the induction of variation potential by burning the leaflet of the first pea leaf. The photosynthetic parameters were calculated on the basis of all photosynthetic responses in the second pea leaf, which were shown in previous work [65].

It was shown that the VP induction by local burning caused a fast decrease in the absolute value of Y(II) (Figure 4a) and increased the absolute value of NPQ (Figure 4b); both changes were significant. The result was in a good agreement with numerous works (e.g., see the review in [5]) devoted to investigating the influence of ESs on photosynthetic processes. The analysis of ΔY(II) and ΔNPQ showed similar changes in the parameters after the VP induction. However, small significant changes in ΔY(II) (decrease) and ΔNPQ (increase) were also observed before the induction of the variation potential. The last result showed slow changes in the investigated photosynthetic parameters (especially, ΔY(II)) before burning, which was in accordance with several works (e.g., [39,40,48,49,87]). The changes were related to the slow photosynthetic response (tens of minutes) induced by illumination with high intensity (probably by the photosynthetic state transition and (or) photodamage).

Figure 5 shows heat maps of Pearson's correlation coefficients of RIs with Y(II) and NPQ and the correlation of ΔRIs with ΔY(II) and ΔNPQ. Only significant correlation coefficients are shown in the figure.
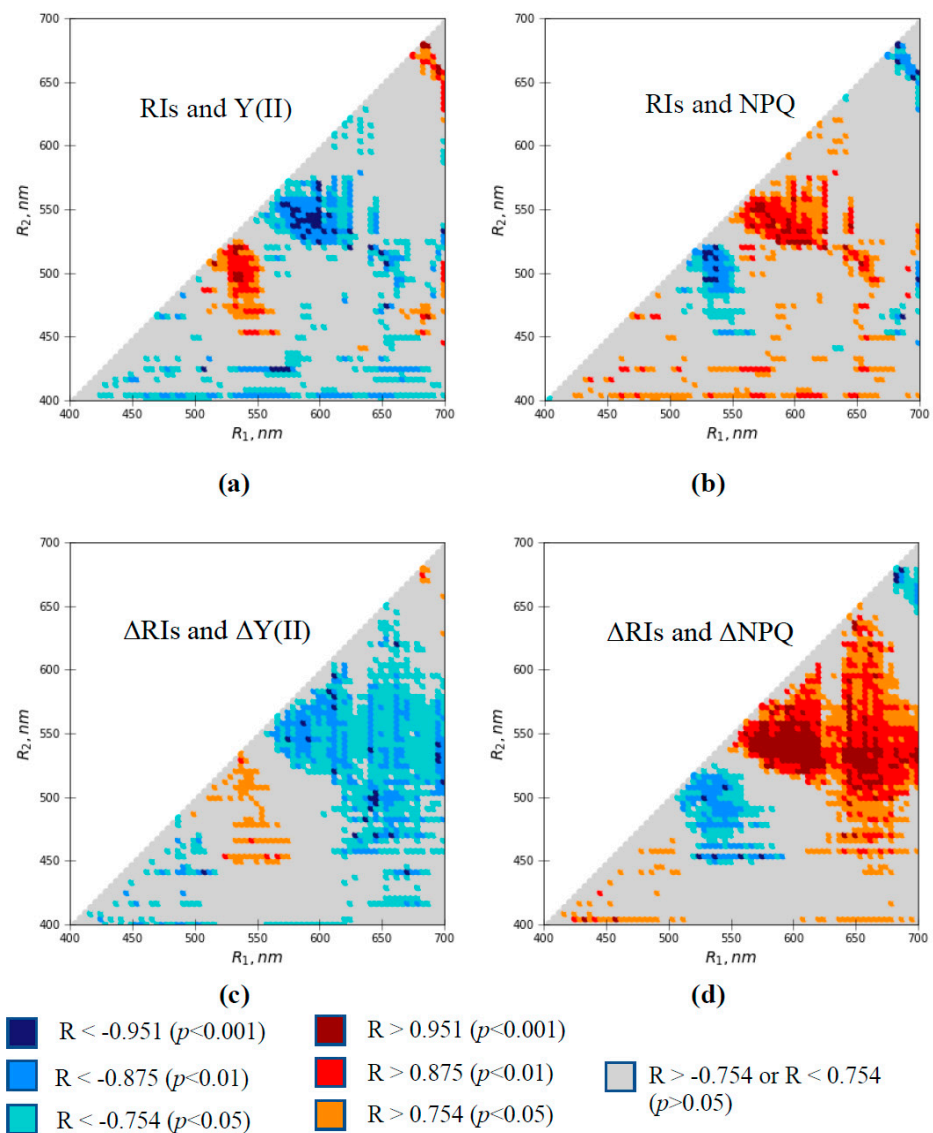
It was shown that both RIs and ΔRIs were strongly correlated to photosynthetic parameters in large spectral regions. In particular, modules of correlation coefficients could be more than 0.95 in several spectral regions (e.g., R_1 is about 595–620 nm and R_2 is about 525–540 nm in Figure 5d). The relations of RIs and ΔRIs to photosynthetic parameters could be positive and negative in different spectral regions. Relationships of reflectance indices to the quantum yield of photosystem II and non-photochemical quenching were mainly opposite, which is in good agreement with the opposing direction of the changes in Y(II) and NPQ (Figure 4).

Areas of the spectral regions with a significant correlation of ΔRIs with ΔY(II) and ΔNPQ were larger than the areas with a significant correlation of RIs with Y(II) and NPQ. The results support the conclusion that the sensitivity of ΔRIs to photosynthetic parameters is higher than the sensitivity of RIs.

Spectral regions with a significant correlation of RIs and ΔRIs with photosynthetic parameters (e.g., R_1 was about 550–620 nm and R_2 was about 500–575 nm, or R_1 was about 510–560 nm and R_2 was about 460–520 nm; Figure 5d) were similar to the spectral regions with significant changes in ΔRIs after the induction of VP (Figure 3). This showed that photosynthetic changes were likely to be the causes of the revealed changes in RIs, which were observed after the induction of the VP in pea leaves.
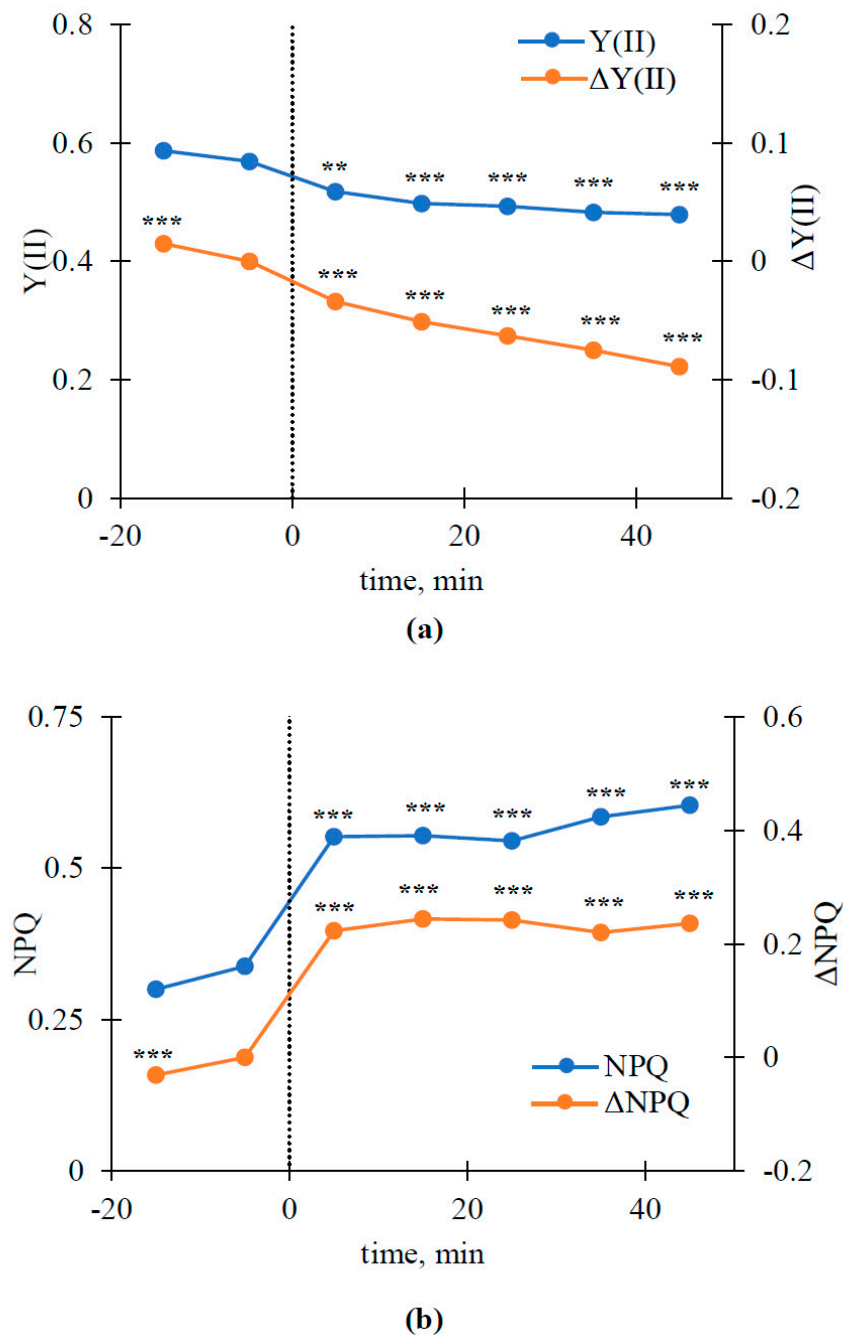
Figure 4. Dynamics of Y(II) and ΔY(II) (**a**) and NPQ and ΔNPQ (**b**) before and after induction of variation potential in the second leaf (*n* = 13). Burning the first leaf was used for VP induction (the burning is marked by the time point zero and dotted line). ΔY(II) and ΔNPQ were calculated as $Y(II)_{TP}$-$Y(II)_C$ and NPQ_{TP}-NPQ_C, respectively. $Y(II)_C$ is the control Y(II) at 5 min before VP induction. $Y(II)_{TP}$ is Y(II) at a specific time point before or after VP induction. NPQ_C is the control NPQ at 5 min before VP induction. NPQ_{TP} is NPQ at a specific time point before or after VP induction. The Mann–Whitney U test was used for *p*-value calculations. Y(II) and NPQ were compared to control values. ΔY(II) and ΔNPQ were compared to zero values (absence of changes). Using ΔY(II) and ΔNPQ minimized the influence of individual plant differences on local burning-induced changes in the parameters. **, $p < 0.01$ and ***, $p < 0.001$.

(a)

(b)

(c)

(d)

R < -0.951 (*p*<0.001)   R > 0.951 (*p*<0.001)

R < -0.875 (*p*<0.01)   R > 0.875 (*p*<0.01)   R > -0.754 or R < 0.754 (*p*>0.05)

R < -0.754 (*p*<0.05)   R > 0.754 (*p*<0.05)

Figure 5. Heat maps of linear correlation coefficients (R) between RIs and Y(II) (**a**), RIs and NPQ (**b**), ΔRIs and ΔY(II) (**c**), and ΔRIs and ΔY(II) (**d**). Pearson's correlation coefficients were calculated based on medians of investigated parameters. The medians were calculated for each time point ($n = 7$). Only significant correlation coefficients are shown in the figure.

3.3. Dynamics of Local Burning-Induced Changes in Some Revealed Reflectance Indices

Furthermore, we analyzed the dynamics of local burning-induced changes in some re-flectance indices, which were included in spectral areas with significant changes (Figure 6). Only ΔRIs were analyzed because changes in the absolute values of RIs were weak. The dynamics of burning-induced changes in ΔRI(571, 542) (R_1 was 571 nm and R_2 was 542 nm), ΔRI(538, 500) (R_1 was 538 nm and R_2 was 500 nm), ΔRI(646, 554) (R_1 was 646 nm and R_2 was 554 nm), and ΔRI(692, 662) (R_1 was 692 nm and R_2 was 662 nm), which were selected on the basis of different spectral ranges in Figure 3, were investigated.

It was shown that all investigated ΔRIs were strongly changed after VP induction. The magnitudes of the changes varied from approximately 0.0025 for ΔRI(571, 542) to 0.007–0.008 for ΔRI(538, 505) and ΔRI(646, 554), similar to the magnitudes of VP-induced changes in PRI [65]. The dynamics of the changes in different ΔRIs also differed: the minimum values of ΔRI(538, 500) and ΔRI(692, 662) were observed at 25 and 5 min after VP induction, respectively. The maximum value of ΔRI(646, 554) was observed at 15 min after

burning. $\Delta RI(571, 542)$ reached maximal values at 5 min after the induction of variation potential, which were weakly changed after that.
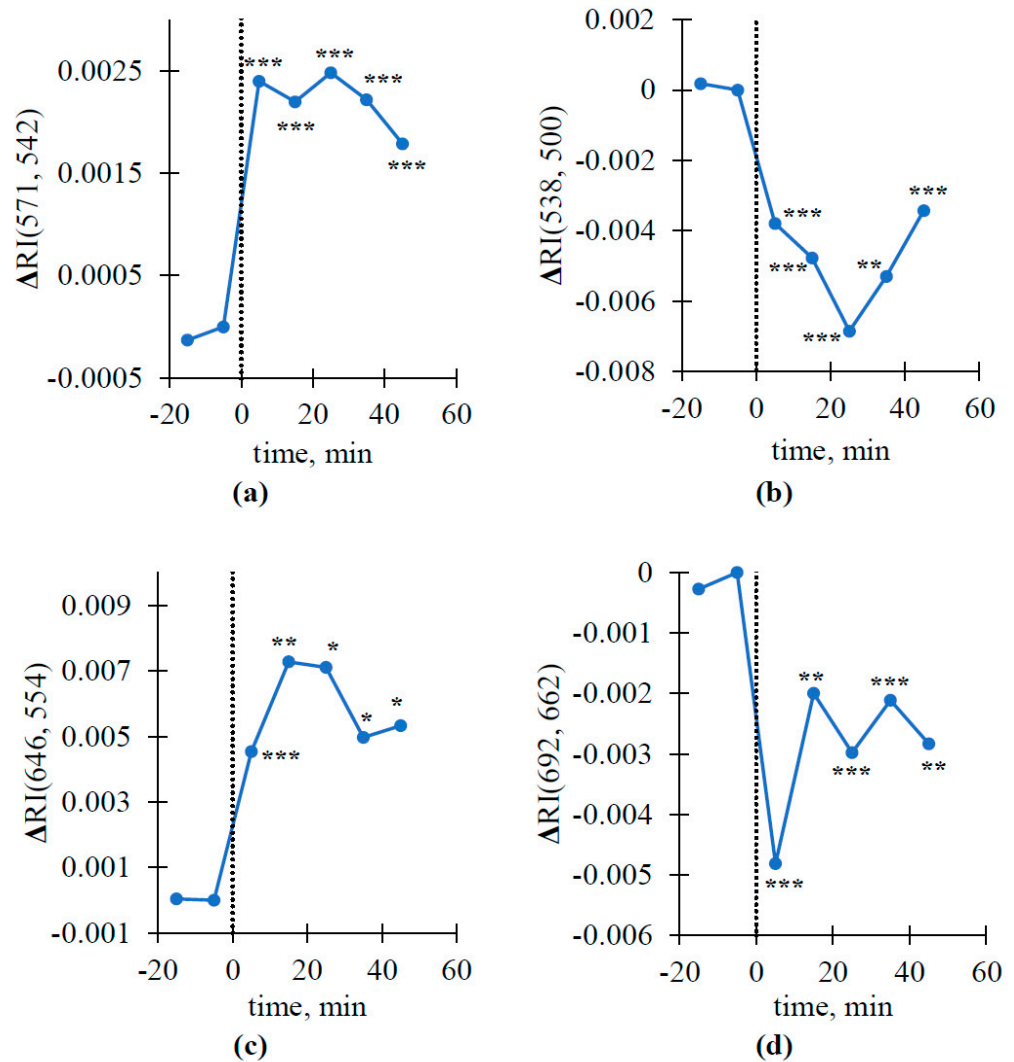
Figure 6. Dynamics of $\Delta RI(571, 542)$ (**a**), $\Delta RI(538, 500)$ (**b**), $\Delta RI(646, 554)$ (**c**), and $\Delta RI(692, 662)$ (**d**) before and after induction of variation potential in the second leaf ($n = 13$). Burning of the first leaf was used for VP induction (the burning is marked by the time point zero and the dotted line). The Mann–Whitney U test was used for *p*-value calculations; parameters were compared to zero values (absence of changes). *, $p < 0.05$, **, $p < 0.01$, and ***, $p < 0.001$.

4. Discussion

Damage-induced VP is a key electrical signal in higher plants influencing numerous physiological processes and, probably, participating in the induction of the systemic adaptive response [2,5,7,8]. Photosynthetic processes are an important target of VP [2,3,5,7,8,27,28,30,31,37–45,48]. Photosynthetic inactivation can be initiated for minutes after VP induction; both dark and light reactions are changed, modifications in photosynthetic processes participate in increasing tolerance of photosynthetic machinery, etc. The VP's influence on photosynthetic processes is based on the pH increase in the apoplast and the pH decrease in the cytoplasm, stroma, and lumen [5,8,38,39,79].

It is known that photosynthetic processes are strongly related to plant optical properties, including fast changes in leaf reflectance (e.g., reflectance in the green spectral range [66,68,75–78,88–90], which is caused by acidification of the lumen of chloroplasts).

Thus, it seems highly probable that VP-induced photosynthetic changes should be accompanied by changes in leaf reflectance, which can potentially be used for their remote sensing.

Our previous results showed that the local burning-induced VP causes changes in broadband reflectance indices and the narrowband water index [63,64], which are related to the water content in leaves, and decrease in the narrowband PRI [65], which is correlated to the quantum yield of photosystems and non-photochemical quenching. Potentially, the VP can induce changes in other difference reflectance indices because the changes are observed under direct actions of stressors (e.g., heating [83]); however, the problem requires an additional complex analysis, such as the analyses in works [80–83]. In the present work, we performed an analysis based on spectral and photosynthetic data, which were obtained from our previous work [65]. We calculated all possible RIs and ΔRIs based on the 400–700 nm spectral range, revealed their changes caused by local burning (the typical inductor of VP [4]), and estimated the relation of the RIs and ΔRIs to the quantum yield of photosystem II and non-photochemical quenching.

The complex analysis shows that the induction of VP by local burning causes significant changes in a large quantity of ΔRIs (Figure 3); in contrast, the changes in RIs were weak (Figure 2). This is in good agreement with results showing that fast changes in PRI (e.g., light-induced [74,76,77,85,86] or VP-induced [65] changes) are more effective estimators of photosynthetic parameters than absolute values of the index. The effect is based on the elimination of individual variability in reflectance spectra related to long-term changes in physiological processes (e.g., content of chlorophylls and carotenoids [71,74]). It is highly likely that a similar mechanism could also decrease errors in our analysis, which is supported by the increased sensitivity of ΔRIs in comparison to the absolute values of RIs in the complex analysis of the spectra of reflected light after short-term heating of plants [83].

Many spectral regions with significant changes in ΔRIs are based in the green and yellow spectral ranges (at least one of two R values is in the 500–600 nm range; Figures 3 and 6); high Pearson's correlation coefficients were also observed in this spectral range (Figure 5). The changes in reflectance indices can be explained by transitions in the xanthophyll cycle because they are sensitive to the photosynthetic decrease in pH in the lumen [88,91,92] and modify reflectance in the 510–560 nm range [66,78]. However, the maximum reflectance was observed at 525–535 nm [66,68,78]. This means that additional mechanisms of change in reflectance in the green and yellow spectral ranges are probable.

Potentially, the mechanisms could be related to light scattering, with maximum values at 530–546 nm, which is dependent on the pH in the lumen (probably through the induction of chloroplast shrinkage [77]) and can influence reflectance [68,75,77,79]. Previously, we showed [79] that light scattering can be stimulated by a VP in peas, and the dynamics of VP-induced changes in light scattering (see, e.g., Figure 7a in [79]) seem to be approximately similar to the dynamics of changes in ΔRI (646, 554) (Figure 6c). It is also known that light scattering is strongly related to NPQ [93,94]; i.e., it should show fast changes in photosynthetic processes.

Another potential mechanism of changes in reflectance can be related to an electrochromic shift in pigment absorbance with maximum values at 515–520 nm [94,95]. The electrochromic shift is caused by electrical potential across thylakoid membranes in chloroplasts [94,95]; this means that this parameter can be also related to photosynthesis. Our earlier results [79] showed that a VP decreases the electrochromic shift in pea leaves, but the magnitude of the decrease is small.

All potential mechanisms (transitions in the xanthophyll cycle, light scattering, and the electrochromic shift) induce changes in ΔRIs as a result of photosynthetic processes, including lumen acidification and formation of electrical potential across thylakoid membranes [92–95]. The correlations between photosynthetic parameters and changes in ΔRIs (Figure 5) support this mechanism.

However, changes in RIs (Figures 3 and 6d) and correlations (Figure 5) were also observed in red spectral regions (R_1 was about 680–700 nm and R_2 was about 645–675 nm).

It should be noted that we cannot divide reflected light itself and fluorescence in the measured reflected light. The maximum photosystem II fluorescence is known to be observed at 685 nm, and chlorophyll absorbance is shown in the blue and red spectral ranges [88]. As a result, we hypothesize that negative changes in ΔRIs based in the red spectral region (see, e.g., Figure 3) show a VP-induced decrease in chlorophyll fluorescence, which is included in $I(R_1)$, in comparison to $I(R_2)$, which is mainly dependent on chlorophyll light absorption. The hypothesis is in good agreement with works [27,37,39,43–45] showing that the non-photochemical quenching of chlorophyll fluorescence can be strongly stimulated by electrical signals [27,37,39,43–45]. The strong negative correlation between RIs (or ΔRIs) and NPQ (or ΔNPQ) in the red spectral range also supports the hypothesis about the participation of the decrease in fluorescence intensity in the VP-induced decrease in RIs based in this spectral region. It should be noted that the VP-induced NPQ increase is also caused by acidification of the chloroplast lumen. The mechanism can contribute to relations between RIs based in the red and green–yellow spectral regions.

Thus, our analysis shows that local burning-induced VP causes changes in a large quantity of ΔRIs, which are mainly related to changes in reflectance in the green and yellow spectral ranges; however, ΔRIs can also be significantly changed in the red spectral range. In the future, these results can provide the basis for the development of new indices for the remote sensing of ES-induced photosynthetic changes in plant leaves. In contrast, absolute values of RIs are weakly changed; i.e., they seem to be weakly effective for revealing the changes induced by VP in higher plants.

5. Materials and Methods

We used the spectra of reflected light and values of photosynthetic parameters (Y(II) and NPQ), which were measured in our earlier work [65]. Details of the experimental procedure were described in the work [65].

Briefly, pea seedlings (*Pisum sativum* L., 14–21 days old) were hydroponically cultivated in a Binder KBW 240 plant growth chamber (Binder GmbH, Tuttlingen, Germany).

VP was induced by burning the leaflet in the first leaf of the pea seedling (flame, 3–4 s, approximately 1 cm^2). The leaflet was burned after 75 min of adaptation of the seedling in the system for measurements of photosynthetic and reflectance parameters.

Photosynthetic and reflectance parameters, which were measured in the second leaves of the pea seedlings, were used in the analysis.

A Pulse-Amplitude-Modulation (PAM) fluorometer Dual-PAM-100 (Heinz Walz GmbH, Effeltrich, Germany) was used for photosynthetic measurements (Y(II) and NPQ). The photosynthetic measurements were initiated after 15 min dark adaptation before turning on the actinic light.

A compact wide-range spectrometer S100 (SOLAR Laser Systems, Minsk, Belarus) and a fiber optics cable were used for measurement of reflected light. The measurements of the reflected light were initiated after 30 min illumination by the actinic light (30 min before VP induction). A white card (QPcard 101 Calibration Card v3, Argraph Corp., Carlstadt, NJ, USA) was used as the reflectance standard for calibration of the reflected light.

A halogen lamp (Osram Decostar, 3000 K, 20 W, 12 V, Germany) was used as the source of the white actinic light. The distance from the lamp to the investigated leaf was approximately 15 cm; the intensity of the leaf illumination by the actinic light was approximately 630 µmol m^{-2} s^{-1}. The duration of illumination before VP induction was 60 min.

Author Contributions: Conceptualization, E.S. and V.S.; methodology, E.S.; software, E.S.; formal analysis, E.S., L.Y., E.G., and A.R.; investigation, L.Y., E.G., A.R., and V.V.; resources, V.V. and V.S.; writing—original draft preparation, E.S. and V.S.; writing—review and editing, V.S.; supervision, V.S.; project administration, V.S.; funding acquisition, V.S. and E.S. All authors have read and agreed to the published version of the manuscript.

References

1. Trebacz, K.; Dziubinska, H.; Krol, E. Electrical signals in long-distance communication in plants. In *Communication in Plants. Neuronal Aspects of Plant Life*; Baluška, F., Mancuso, S., Volkmann, D., Eds.; Springer: Berlin/Heidelberg, Germany; New York, NY, USA, 2006; pp. 277–290.
2. Fromm, J.; Lautner, S. Electrical signals and their physiological significance in plants. *Plant Cell Environ.* **2007**, *30*, 249–257. [CrossRef]
3. Gallé, A.; Lautner, S.; Flexas, J.; Fromm, J. Environmental stimuli and physiological responses: The current view on electrical signaling. *Environ. Exp. Bot.* **2015**, *114*, 15–21. [CrossRef]
4. Vodeneev, V.; Akinchits, E.; Sukhov, V. Variation potential in higher plants: Mechanisms of generation and propagation. *Plant Signal. Behav.* **2015**, *10*, e1057365. [CrossRef] [PubMed]
5. Sukhov, V. Electrical signals as mechanism of photosynthesis regulation in plants. *Photosynth. Res.* **2016**, *130*, 373–387. [CrossRef] [PubMed]
6. Sukhova, E.; Akinchits, E.; Sukhov, V. Mathematical models of electrical activity in plants. *J. Membr. Biol.* **2017**, *250*, 407–423. [CrossRef] [PubMed]
7. Szechyńska-Hebda, M.; Lewandowska, M.; Karpiński, S. Electrical signaling, photosynthesis and systemic acquired acclimation. *Front. Physiol.* **2017**, *8*, 684. [CrossRef] [PubMed]
8. Sukhov, V.; Sukhova, E.; Vodeneev, V. Long-distance electrical signals as a link between the local action of stressors and the systemic physiological responses in higher plants. *Progr. Biophys. Mol. Biol.* **2019**, *146*, 63–84. [CrossRef]
9. Farmer, E.E.; Gao, Y.Q.; Lenzoni, G.; Wolfender, J.L.; Wu, Q. Wound- and mechanostimulated electrical signals control hormone responses. *New Phytol.* **2020**, *227*, 1037–1050. [CrossRef]
10. Felle, H.H.; Zimmermann, M.R. Systemic signalling in barley through action potentials. *Planta* **2007**, *226*, 203–214. [CrossRef]
11. Zimmermann, M.R.; Maischak, H.; Mithöfer, A.; Boland, W.; Felle, H.H. System potentials, a novel electrical long-distance apoplastic signal in plants, induced by wounding. *Plant Physiol.* **2009**, *149*, 1593–1600. [CrossRef]
12. Zimmermann, M.R.; Mithöfer, A.; Will, T.; Felle, H.H.; Furch, A.C. Herbivore-triggered electrophysiological reactions: Candidates for systemic signals in higher plants and the challenge of their identification. *Plant Physiol.* **2016**, *170*, 2407–2419. [CrossRef]
13. Stahlberg, R.; Cleland, R.E.; van Volkenburgh, E. Slow wave potentials—A propagating electrical signal unique to higher plants. In *Communication in Plants. Neuronal Aspects of Plant Life*; Baluška, F., Mancuso, S., Volkmann, D., Eds.; Springer: Berlin/Heidelberg, Germany; New York, NY, USA, 2006; pp. 291–308.
14. Stahlberg, R.; Cosgrove, D.J. The propagation of slow wave potentials in pea epicotyls. *Plant Physiol.* **1997**, *113*, 209–217. [CrossRef] [PubMed]
15. Mancuso, S. Hydraulic and electrical transmission of wound-induced signals in *Vitis vinifera*. *Aust. J. Plant Physiol.* **1999**, *26*, 55–61. [CrossRef]
16. Sukhova, E.; Akinchits, E.; Gudkov, S.V.; Pishchalnikov, R.Y.; Vodeneev, V.; Sukhov, V. A theoretical analysis of relations between pressure changes along xylem vessels and propagation of variation potential in higher plants. *Plants* **2021**, *10*, 372. [CrossRef] [PubMed]
17. Toyota, M.; Spencer, D.; Sawai-Toyota, S.; Jiaqi, W.; Zhang, T.; Koo, A.J.; Howe, G.A.; Gilroy, S. Glutamate triggers long-distance, calcium-based plant defense signaling. *Science* **2018**, *361*, 1112–1115. [CrossRef] [PubMed]
18. Malone, M. Wound-induced hydraulic signals and stimulus transmission in *Mimosa pudica* L. *New Phytol.* **1994**, *128*, 49–56. [CrossRef] [PubMed]
19. Evans, M.J.; Morris, R.J. Chemical agents transported by xylem mass flow propagate variation potentials. *Plant J.* **2017**, *91*, 1029–1037. [CrossRef] [PubMed]
20. Vodeneev, V.; Mudrilov, M.; Akinchits, E.; Balalaeva, I.; Sukhov, V. Parameters of electrical signals and photosynthetic responses induced by them in pea seedlings depend on the nature of stimulus. *Funct. Plant Biol.* **2018**, *45*, 160–170. [CrossRef]

21. Blyth, M.G.; Morris, R.J. Shear-enhanced dispersion of a wound substance as a candidate mechanism for variation potential transmission. *Front. Plant Sci.* **2019**, *10*, 1393. [CrossRef]

22. Wildon, D.C.; Thain, J.F.; Minchin, P.E.H.; Gubb, I.R.; Reilly, A.J.; Skipper, Y.D.; Doherty, H.M.; O'Donnell, P.J.; Bowles, D. Electrical signalling and systemic proteinase inhibitor Induction in the wounded plant. *Nature* **1992**, *360*, 62–65. [CrossRef]

23. Peña-Cortés, H.; Fisahn, J.; Willmitzer, L. Signals involved in wound-induced proteinase inhibitor II gene expression in tomato and potato plants. *Proc. Natl. Acad. Sci. USA* **1995**, *92*, 4106–4113. [CrossRef]

24. Stanković, B.; Davies, E. Both action potentials and variation potentials induce proteinase inhibitor gene expression in tomato. *FEBS Lett.* **1996**, *390*, 275–279. [CrossRef]

25. Mousavi, S.A.; Chauvin, A.; Pascaud, F.; Kellenberger, S.; Farmer, E.E. GLUTAMATE RECEPTOR-LIKE genes mediate leaf-to-leaf wound signalling. *Nature* **2013**, *500*, 422–426. [CrossRef]

26. Filek, M.; Kościelniak, J. The effect of wounding the roots by high temperature on the respiration rate of the shoot and propagation of electric signal in horse bean seedlings (*Vicia faba* L. minor). *Plant Sci.* **1997**, *123*, 39–46. [CrossRef]

27. Pavlovič, A.; Slováková, L.; Pandolfi, C.; Mancuso, S. On the mechanism underlying photosynthetic limitation upon trigger hair irritation in the carnivorous plant Venus flytrap (*Dionaea muscipula* Ellis). *J. Exp. Bot.* **2011**, *62*, 1991–2000. [CrossRef]

28. Surova, L.; Sherstneva, O.; Vodeneev, V.; Katicheva, L.; Semina, M.; Sukhov, V. Variation potential-induced photosynthetic and respiratory changes increase ATP content in pea leaves. *J. Plant Physiol.* **2016**, *202*, 57–64. [CrossRef] [PubMed]

29. Lautner, S.; Stummer, M.; Matyssek, R.; Fromm, J.; Grams, T.E.E. Involvement of respiratory processes in the transient knockout of net CO_2 uptake in *Mimosa pudica* upon heat stimulation. *Plant Cell Environ.* **2014**, *37*, 254–260. [CrossRef]

30. Hlaváčková, V.; Krchňák, P.; Naus, J.; Novák, O.; Spundová, M.; Strnad, M. Electrical and chemical signals involved in short-term systemic photosynthetic responses of tobacco plants to local burning. *Planta* **2006**, *225*, 235–244. [CrossRef] [PubMed]

31. Krausko, M.; Perutka, Z.; Šebela, M.; Šamajová, O.; Šamaj, J.; Novák, O.; Pavlovič, A. The role of electrical and jasmonate signalling in the recognition of captured prey in the carnivorous sundew plant *Drosera capensis*. *New Phytol.* **2017**, *213*, 1818–1835. [CrossRef] [PubMed]

32. Pavlovič, A.; Mithöfer, A. Jasmonate signalling in carnivorous plants: Copycat of plant defence mechanisms. *J. Exp. Bot.* **2019**, *70*, 3379–3389. [CrossRef]

33. Fromm, J. Control of phloem unloading by action potentials in Mimosa. *Physiol. Plant* **1991**, *83*, 529–533. [CrossRef]

34. Furch, A.C.; van Bel, A.J.; Fricker, M.D.; Felle, H.H.; Fuchs, M.; Hafke, J.B. Sieve element Ca^{2+} channels as relay stations between remote stimuli and sieve tube occlusion in *Vicia faba*. *Plant Cell.* **2009**, *21*, 2118–2132. [CrossRef]

35. Furch, A.C.; Zimmermann, M.R.; Will, T.; Hafke, J.B.; van Bel, A.J. Remote-controlled stop of phloem mass flow by biphasic occlusion in *Cucurbita maxima*. *J. Exp. Bot.* **2010**, *61*, 3697–3708. [CrossRef] [PubMed]

36. Shiina, T.; Tazawa, M. Action potential in *Luffa cylindrica* and its effects on elongation growth. *Plant Cell Physiol.* **1986**, *27*, 1081–1089.

37. Krupenina, N.A.; Bulychev, A.A. Action potential in a plant cell lowers the light requirement for non-photochemical energy-dependent quenching of chlorophyll fluorescence. *Biochim. Biophys. Acta* **2007**, *1767*, 781–788. [CrossRef] [PubMed]

38. Grams, T.E.; Lautner, S.; Felle, H.H.; Matyssek, R.; Fromm, J. Heat-induced electrical signals affect cytoplasmic and apoplastic pH as well as photosynthesis during propagation through the maize leaf. *Plant Cell Environ.* **2009**, *32*, 319–326. [CrossRef]

39. Sukhov, V.; Sherstneva, O.; Surova, L.; Katicheva, L.; Vodeneev, V. Proton cellular influx as a probable mechanism of variation potential influence on photosynthesis in pea. *Plant Cell Environ.* **2014**, *37*, 2532–2541. [CrossRef]

40. Gallé, A.; Lautner, S.; Flexas, J.; Ribas-Carbo, M.; Hanson, D.; Roesgen, J.; Fromm, J. Photosynthetic responses of soybean (*Glycine max* L.) to heat-induced electrical signalling are predominantly governed by modifications of mesophyll conductance for CO_2. *Plant Cell Environ.* **2013**, *36*, 542–552. [CrossRef]

41. Vuralhan-Eckert, J.; Lautner, S.; Fromm, J. Effect of simultaneously induced environmental stimuli on electrical signalling and gas exchange in maize plants. *J. Plant Physiol.* **2018**, *223*, 32–36. [CrossRef]

42. Yudina, L.; Sukhova, E.; Sherstneva, O.; Grinberg, M.; Ladeynova, M.; Vodeneev, V.; Sukhov, V. Exogenous abscisic acid can influence photosynthetic processes in peas through a decrease in activity of H^+-ATPase in the plasma membrane. *Biology* **2020**, *9*, 324. [CrossRef]

43. Yudina, L.; Sherstneva, O.; Sukhova, E.; Grinberg, M.; Mysyagin, S.; Vodeneev, V.; Sukhov, V. Inactivation of H+-ATPase participates in the influence of variation potential on photosynthesis and respiration in peas. *Plants* **2020**, *9*, 1585. [CrossRef]

44. Sukhov, V.; Surova, L.; Sherstneva, O.; Katicheva, L.; Vodeneev, V. Variation potential influence on photosynthetic cyclic electron flow in pea. *Front. Plant Sci.* **2015**, *5*, 766. [CrossRef]

45. Sukhova, E.; Mudrilov, M.; Vodeneev, V.; Sukhov, V. Influence of the variation potential on photosynthetic flows of light energy and electrons in pea. *Photosynth. Res.* **2018**, *136*, 215–228. [CrossRef] [PubMed]

46. Retivin, V.G.; Opritov, V.A.; Fedulina, S.B. Generation of action potential induces preadaptation of Cucurbita pepo L. stem tissues to freezing injury. *Russ. J. Plant Physiol.* **1997**, *44*, 432–442.

47. Retivin, V.G.; Opritov, V.A.; Lobov, S.A.; Tarakanov, S.A.; Khudyakov, V.A. Changes in the resistance of photosynthesizing cotyledon cells of pumpkin seedlings to cooling and heating, as induced by the stimulation of the root system with KCl solution. *Russ. J. Plant Physiol.* **1999**, *46*, 689–696.

48. Sukhov, V.; Surova, L.; Sherstneva, O.; Vodeneev, V. Influence of variation potential on resistance of the photosynthetic machinery to heating in pea. *Physiol. Plant* **2014**, *152*, 773–783. [CrossRef]

49. Sukhov, V.; Surova, L.; Sherstneva, O.; Bushueva, A.; Vodeneev, V. Variation potential induces decreased PSI damage and increased PSII damage under high external temperatures in pea. *Funct. Plant Biol.* **2015**, *42*, 727–736. [CrossRef]

50. Surova, L.; Sherstneva, O.; Vodeneev, V.; Sukhov, V. Variation potential propagation decreases heat-related damage of pea photosystem I by 2 different pathways. *Plant Sign. Behav.* **2016**, *11*, e1145334. [CrossRef]

51. Sukhov, V.; Gaspirovich, V.; Mysyagin, S.; Vodeneev, V. High-temperature tolerance of photosynthesis can be linked to local electrical responses in leaves of pea. *Front. Physiol.* **2017**, *8*, 763. [CrossRef]

52. Suzuki, N.; Miller, G.; Salazar, C.; Mondal, H.A.; Shulaev, E.; Cortes, D.F.; Shuman, J.L.; Luo, X.; Shah, J.; Schlauch, K.; et al. Temporal-spatial interaction between reactive oxygen species and abscisic acid regulates rapid systemic acclimation in plants. *Plant Cell.* **2013**, *25*, 3553–3569. [CrossRef]

53. Souza, G.M.; Ferreira, A.S.; Saraiva, G.F.; Toledo, G.R. Plant "electrome" can be pushed toward a self-organized critical state by external cues: Evidences from a study with soybean seedlings subject to different environmental conditions. *Plant Signal Behav.* **2017**, *12*, e1290040. [CrossRef] [PubMed]

54. Saraiva, G.F.R.; Ferreira, A.S.; Souza, G.M. Osmotic stress decreases complexity underlying the electrophysiological dynamic in soybean. *Plant Biol.* **2017**, *19*, 702–708. [CrossRef]

55. Debono, M.W.; Souza, G.M. Plants as electromic plastic interfaces: A mesological approach. *Prog. Biophys. Mol. Biol.* **2019**, *146*, 123–133. [CrossRef] [PubMed]

56. Simmi, F.Z.; Dallagnol, L.J.; Ferreira, A.S.; Pereira, D.R.; Souza, G.M. Electrome alterations in a plant-pathogen system: Toward early diagnosis. *Bioelectrochemistry* **2020**, *133*, 107493. [CrossRef] [PubMed]

57. Parise, A.G.; Reissig, G.N.; Basso, L.F.; Senko, L.G.S.; Oliveira, T.F.C.; de Toledo, G.R.A.; Ferreira, A.S.; Souza, G.M. Detection of different hosts from a distance alters the behaviour and bioelectrical activity of *Cuscuta racemosa*. *Front. Plant Sci.* **2021**, *12*, 594195. [CrossRef] [PubMed]

58. Chatterjee, S.K.; Ghosh, S.; Das, S.; Manzella, V.; Vitaletti, A.; Masi, E.; Santopolo, L.; Mancuso, S.; Maharatna, K. Forward and inverse modelling approaches for prediction of light stimulus from electrophysiological response in plants. *Measurement* **2014**, *53*, 101–116. [CrossRef]

59. Chatterjee, S.K.; Das, S.; Maharatna, K.; Masi, E.; Santopolo, L.; Mancuso, S.; Vitaletti, A. Exploring strategies for classification of external stimuli using statistical features of the plant electrical response. *J. R. Soc. Interface* **2015**, *12*, 20141225. [CrossRef]

60. Chen, Y.; Zhao, D.-J.; Wang, Z.-Y.; Wang, Z.-Y.; Tang, G.; Huang, L. Plant electrical signal classification based on waveform similarity. *Algorithms* **2016**, *9*, 70. [CrossRef]

61. Chatterjee, S.K.; Malik, O.; Gupta, S. Chemical sensing employing plant electrical signal response-classification of stimuli using curve fitting coefficients as features. *Biosensors* **2018**, *8*, 83. [CrossRef]

62. Qin, X.-H.; Wang, Z.-Y.; Yao, J.-P.; Zhou, Q.; Zhao, P.-F.; Wang, Z.-Y.; Huang, L. Using a one-dimensional convolutional neural network with a conditional generative adversarial network to classify plant electrical signals. *Comp. Electron. Agric.* **2020**, *174*, 105464. [CrossRef]

63. Sukhova, E.; Yudina, L.; Akinchits, E.; Vodeneev, V.; Sukhov, V. Influence of electrical signals on pea leaf reflectance in the 400-800-nm range. *Plant Signal. Behav.* **2019**, *14*, 1610301. [CrossRef]

64. Sukhova, E.; Yudina, L.; Gromova, E.; Nerush, V.; Vodeneev, V.; Sukhov, V. Burning-induced electrical signals influence broadband reflectance indices and water index in pea leaves. *Plant Signal. Behav.* **2020**, *15*, 1737786. [CrossRef]

65. Sukhov, V.; Sukhova, E.; Gromova, E.; Surova, L.; Nerush, V.; Vodeneev, V. The electrical signal-induced systemic photosynthetic response is accompanied by changes in the photochemical reflectance index in pea. *Func. Plant Biol.* **2019**, *46*, 328–338. [CrossRef] [PubMed]

66. Gamon, J.A.; Peñuelas, J.; Field, C.B. A narrow-waveband spectral index that tracks diurnal changes in photosynthetic efficiency. *Remote Sens. Environ.* **1992**, *41*, 35–44. [CrossRef]

67. Filella, I.; Amaro, T.; Araus, J.L.; Peñuelas, J. Relationship between photosynthetic radiation-use efficiency of barley canopies and the photochemical reflectance index (PRI). *Physiol. Plant.* **1996**, *96*, 211–216. [CrossRef]

68. Gamon, J.A.; Serrano, L.; Surfus, J.S. The photochemical reflectance index: An optical indicator of photosynthetic radiation use efficiency across species, functional types, and nutrient levels. *Oecologia* **1997**, *112*, 492–501. [CrossRef] [PubMed]

69. Garbulsky, M.F.; Peñuelas, J.; Gamon, J.; Inoue, Y.; Filella, I. The photochemical reflectance index (PRI) and the remote sensing of leaf, canopy and ecosystem radiation use efficiencies. A review and meta-analysis. *Remote Sens. Environ.* **2011**, *115*, 281–297. [CrossRef]

70. Peñuelas, J.; Garbulsky, M.F.; Filella, I. Photochemical reflectance index (PRI) and remote sensing of plant CO_2 uptake. *New Phytol.* **2011**, *191*, 596–599. [CrossRef]

71. Porcar-Castell, A.; Garcia-Plazaola, J.I.; Nichol, C.J.; Kolari, P.; Olascoaga, B.; Kuusinen, N.; Fernández-Marín, B.; Pulkkinen, M.; Juurola, E.; Nikinmaa, E. Physiology of the seasonal relationship between the photochemical reflectance index and photosynthetic light use efficiency. *Oecologia* **2012**, *170*, 313–323. [CrossRef]

72. Zhang, C.; Filella, I.; Garbulsky, M.F.; Peñuelas, J. Affecting factors and recent improvements of the photochemical reflectance index (PRI) for remotely sensing foliar, canopy and ecosystemic radiation-use efficiencies. *Remote Sens.* **2016**, *8*, 677. [CrossRef]

73. Sukhova, E.; Sukhov, V. Connection of the photochemical reflectance index (PRI) with the photosystem II quantum yield and nonphotochemical quenching can be dependent on variations of photosynthetic parameters among investigated plants: A meta-analysis. *Remote Sens.* **2018**, *10*, 771. [CrossRef]

74. Kováč, D.; Veselá, B.; Klem, K.; Večeřová, K.; Kmecová, Z.M.; Peñuelas, J.; Urban, O. Correction of PRI for carotenoid pigment pools improves photosynthesis estimation across different irradiance and temperature conditions. *Remote Sens. Environ.* **2020**, *244*, 111834. [CrossRef]

75. Evain, S.; Flexas, J.; Moya, I. A new instrument for passive remote sensing: 2. Measurement of leaf and canopy reflectance changes at 531 nm and their relationship with photosynthesis and chlorophyll fluorescence. *Remote Sens. Environ.* **2004**, *91*, 175–185. [CrossRef]

76. Sukhova, E.; Sukhov, V. Analysis of light-induced changes in the photochemical reflectance index (PRI) in leaves of pea, wheat, and pumpkin using pulses of green-yellow measuring light. *Remote Sens.* **2019**, *11*, 810. [CrossRef]

77. Sukhova, E.; Sukhov, V. Relation of photochemical reflectance indices based on different wavelengths to the parameters of light reactions in photosystems I and II in pea plants. *Remote Sens.* **2020**, *12*, 1312. [CrossRef]

78. Van Wittenberghe, S.; Laparra, V.; García-Plazaola, J.I.; Fernández-Marín, B.; Porcar-Castell, A.; Moreno, J. Combined dynamics of the 500-600 nm leaf absorption and chlorophyll fluorescence changes in vivo: Evidence for the multifunctional energy quenching role of xanthophylls. *Biochim. Biophys. Acta Bioenergy* **2021**, *1862*, 148351. [CrossRef]

79. Sukhov, V.; Surova, L.; Morozova, E.; Sherstneva, O.; Vodeneev, V. Changes in H^+-ATP synthase activity, proton electrochemical gradient, and pH in pea chloroplast can be connected with variation potential. *Front Plant Sci.* **2016**, *7*, 1092. [CrossRef]

80. Balzarolo, M.; Peñuelas, J.; Filella, I.; Portillo-Estrada, M.; Ceulemans, R. Assessing ecosystem isoprene emissions by hyperspectral remote sensing. *Remote Sens.* **2018**, *10*, 1086. [CrossRef]

81. Sytar, O.; Brücková, K.; Kovár, M.; Živčák, M.; Hemmerich, I.; Brestič, M. Nondestructive detection and biochemical quantification of buckwheat leaves using visible (VIS) and near-infrared (NIR) hyperspectral reflectance imaging. *J. Centr. Eur. Agric.* **2017**, *18*, 864–878. [CrossRef]

82. Sun, H.; Feng, M.; Xiao, L.; Yang, W.; Wang, C.; Jia, X.; Zhao, Y.; Zhao, C.; Muhammad, S.K.; Li, D. Assessment of plant water status in winter wheat (*Triticum aestivum L.*) based on canopy spectral indices. *PLoS ONE* **2019**, *14*, e0216890. [CrossRef] [PubMed]

83. Sukhova, E.; Yudina, L.; Gromova, E.; Ryabkova, A.; Kior, D.; Sukhov, V. Complex analysis of the efficiency of difference reflectance indices on the basis of 400–700 nm wavelengths for revealing the influences of water shortage and heating on plant seedlings. *Remote Sens.* **2021**, *13*, 962. [CrossRef]

84. Ibaraki, Y.; Dutta Gupta, S. Nondestructive evaluation of the photosynthetic properties of micropropagated plantlets by imaging photochemical reflectance index under low light intensity. *In Vitro Cell. Dev. Biol. Plant.* **2010**, *46*, 530–536. [CrossRef]

85. Yudina, L.; Sukhova, E.; Gromova, E.; Nerush, V.; Vodeneev, V.; Sukhov, V. A light-induced decrease in the photochemical reflectance index (PRI) can be used to estimate the energy-dependent component of non-photochemical quenching under heat stress and soil drought in pea, wheat, and pumpkin. *Photosynth. Res.* **2020**, *146*, 175–187. [CrossRef] [PubMed]

86. Kováč, D.; Veselovská, P.; Klem, K.; Večeřová, K.; Ač, A.; Peñuelas, J.; Urban, O. Potential of photochemical reflectance index for indicating photochemistry and light use efficiency in leaves of *European beech* and *Norway spruce* trees. *Remote Sens.* **2018**, *10*, 1202. [CrossRef]

87. Białasek, M.; Górecka, M.; Mittler, R.; Karpiński, S. Evidence for the Involvement of electrical, calcium and ROS signaling in the systemic regulation of non-photochemical quenching and photosynthesis. *Plant Cell Physiol.* **2017**, *58*, 207–215. [CrossRef] [PubMed]

88. Porcar-Castell, A.; Tyystjärvi, E.; Atherton, J.; van der Tol, C.; Flexas, J.; Pfündel, E.E.; Moreno, J.; Frankenberg, C.; Berry, J.A. Linking chlorophyll a fluorescence to photosynthesis for remote sensing applications: Mechanisms and challenges. *J. Exp. Bot.* **2014**, *65*, 4065–4095. [CrossRef]

89. Kohzuma, K.; Hikosaka, K. Physiological validation of photochemical reflectance index (PRI) as a photosynthetic parameter using *Arabidopsis thaliana* mutants. *Biochem. Biophys. Res. Commun.* **2018**, *498*, 52–57. [CrossRef]

90. Murakami, K.; Ibaraki, Y. Time course of the photochemical reflectance index during photosynthetic induction: Its relationship with the photochemical yield of photosystem II. *Physiol. Plant.* **2019**, *165*, 524–536. [CrossRef]

91. Müller, P.; Li, X.P.; Niyogi, K.K. Non-photochemical quenching. A response to excess light energy. *Plant Physiol.* **2001**, *125*, 1558–1566. [CrossRef]

92. Ruban, A.V. Nonphotochemical chlorophyll fluorescence quenching: Mechanism and effectiveness in protecting plants from photodamage. *Plant Physiol.* **2016**, *170*, 1903–1916. [CrossRef]

93. Ruban, A.V.; Pascal, A.A.; Robert, B.; Horton, P. Activation of zeaxanthin is an obligatory event in the regulation of photosynthetic light harvesting. *J. Biol. Chem.* **2002**, *277*, 7785–7789. [CrossRef] [PubMed]

94. Schreiber, U.; Klughammer, C. New accessory for the DUAL-PAM-100: The P515/535 module and examples of its application. *PAM Appl. Notes.* **2008**, *1*, 1–10.

95. Klughammer, C.; Siebke, K.; Schreiber, U. Continuous ECS-indicated recording of the proton-motive charge flux in leaves. *Photosynth Res.* **2013**, *117*, 471–487. [CrossRef] [PubMed]